Astrophysical Journal - Submitted.

Coronal element abundances of the post-common envelope binary V471 Tauri with *ASCA*

Martin Still[1]
NASA/Goddard Space Flight Center, Code 662, Greenbelt, MD 20771

Gaitee Hussain
Harvard-Smithsonian Center for Astrophysics, 60 Garden Street, Cambridge, MA 02138

ABSTRACT

We report on *ASCA* observations of the coronally active companion star in the post-common envelope binary V471 Tau. While it would be prudent to check the following results with grating spectroscopy, we find that a single-temperature plasma model does not fit the data. Two-temperature models with variable abundances indicate that Fe is underabundant compared to the Hyades photospheric mean, whereas, the high first ionization potential element Ne is overabundant. This is indicative of the inverse first ionization effect, believed to result from the fractionation of ionized material by the magnetic field in the upper atmosphere of the star. Evolutionary calculations indicate that there should be no peculiar abundances on the companion star resulting from the common envelope epoch. Indeed, we find no evidence for peculiar abundances, although uncertainties are high.

Subject headings: binaries: close – stars: individual: V471 Tau – stars: magnetic fields – stars: white dwarfs – X-rays: binaries

1. Introduction

CCD and Proportional Counter spectroscopy of stellar coronal plasmas has revealed multi-temperature environments with a variety of abundance distributions over ionization potential. However, because of the moderate spectral resolutions available, combined with the confusion of line blending, much has been made of the possible ambiguity in abundance measurements (Drake 1996). The grating spectrographs recently launched on the *XMM-Newton* and *Chandra* satellites have confirmed the general results of lower-resolution spectroscopy (Brinkman et al. 2001; Audard et al. 2001). Consequently, despite statistical uncertainties larger than the grating cameras and the possibility of line confusion, confidence in CCD and Proportional Counter measurements has improved. In this paper we present *ASCA* spectroscopy of the relatively faint coronal source V471 Tau.

V471 Tau is a 12.5 hour eclipsing binary with a white dwarf and K2 companion (Nelson and Young 1970). At a distance of 47 pc (Werner & Rauch 1997), it is the closest object which has been through a recent common envelope phase of evolution. During the red giant phase of the white dwarf progenitor's life, the envelope of the giant was large enough to contain the orbit of the K star companion. While the two stars shared a common envelope, tides, friction and mass loss created a significantly smaller binary, with a short orbital period (Paczýnksi 1976). The envelope of the giant has since been ejected, but the binary still loses angular momentum through wind braking and gravitational radiation (Taam 1983). V471 Tau is therefore one of the best candidates for a pre-cataclysmic variable (pre-CV). CVs occur when the orbital period of a white dwarf–red

[1]Universities Space Research Association

dwarf binary becomes short enough for the main-sequence companion to fill it's Roche lobe. Quasi-persistent accretion will then occur through Roche lobe overflow. These objects are the sources of dwarf nova outbursts and classical nova eruptions that enrich the galactic ISM (Warner 1995).

Soft X-rays from V471 Tau were discovered by HEAO 1 (van Buren, Charles & Mason 1980) and it was detected as a flaring source by the *Einstein* Observatory (Young et al. 1983). Jensen et al. (1986) used *EXOSAT* to find white dwarf eclipses, orbital dips and emission from both stellar components. Wheatley (1998) employed *ROSAT* to identify the K star from the white dwarf spectrally and pointed out that the K star flux was brighter than the average Hyades member but similar to the younger, faster rotators of the Pleiades. Therefore coronal luminosity in this source is probably related to rotation rate rather than age.

With model assumptions, we show in this paper that the coronal abundances of a sample of metals are statistically significant, where Fe is under-abundant relative to the mean photospheric Hyades content and Ne is over-abundant, at least relative to the solar photosphere. This suggests that there is an ionization-dependent fractionation process in the upper atmosphere of the star, as indicated in other coronal sources more robustly by the grating cameras on *XMM-Newton* and *Chandra*.

2. Observations

The Advanced Satellite for Cosmology and Astrophysics (*ASCA*; Tanaka, Inoue & Holt 1994) comprised four identical telescopes of nested thin foil reflectors (Serlemitsos et al. 1995). Four cameras were mounted at the focal planes. Two had Solid state Imaging Spectrometers (SIS0 and SIS1); Burke et al. 1991), and two carried Gas Imaging Spectrometers (GIS2 and GIS3) which were scintillation proportional counters (Ohashi et al. 1991). Between MJD 50321.75 and MJD 50322.90, *ASCA* was pointed at V471 Tau for a total exposure time of 50 ksec, over 17 near-contiguous orbits. The ASCA sequence number of the observations is 24032000. The SIS cameras operated in BRIGHT mode while GIS data was taken in PH mode with normal bit assignments.

3. Analysis

Observations were screened using standard criteria in FTOOLS v5.1, excluding time intervals of South Atlantic Anomaly, Earth Occultation and bright Earth limb. Hot and flickering pixels were removed from the SIS events and we rejected particle events from the GIS observations. A total of 44 ksec of good data remained. The hot white dwarf component is softer than the *ASCA* energy band (Wheatley 1998), we find no evidence for it in the current data, and therefore we do not consider it in the following analysis.

3.1. Photometry

SIS event rates were determined within two spatially-distinct, circular region masks of diameter 8 arcmin and 5 arcmin for the source and background, respectively. Source events were extracted from the GIS tables within a circular region 12 arcmin in diameter and a background annulus 12–24 arcmin from the target. Background rates were normalized by the appropriate ratio of extraction areas and subtracted from the source events. The total SIS+GIS source event rate during the observation is provided in Fig. 1, averaged without weights into 1 ksec bins. We also provide the hardness ratio in the bands 0.3–1.0 keV and 1.0–10.0 keV.

Count rate is approximately constant, except for three flares, each of duration a few thousand ksec. Statistically, the shape of the flares are not well-defined and there is only marginal evidence for spectral hardening, but their durations are more akin to long-decay flares (Tsikoudi & Kellet 2000) rather than the short, impulsive variety (Schmitt, Haisch & Barwig 1993). V471 Tau is relatively faint compared to most well-observed coronal sources (e.g. Brinkman et al. 2001, Audard 2001), so in order to maximize counting statistics during spectral fitting, we do not separate flare events from the quiescent data.

3.2. Spectroscopy

To allow accurate χ^2 fitting, spectral channels containing less that 30 events were binned with their neighbors. Events flagged as bad were rejected and those with corrected pulse heights of $E > 10$ keV were ignored. Best fits to the data were determined using the VAPEC thermal plasma

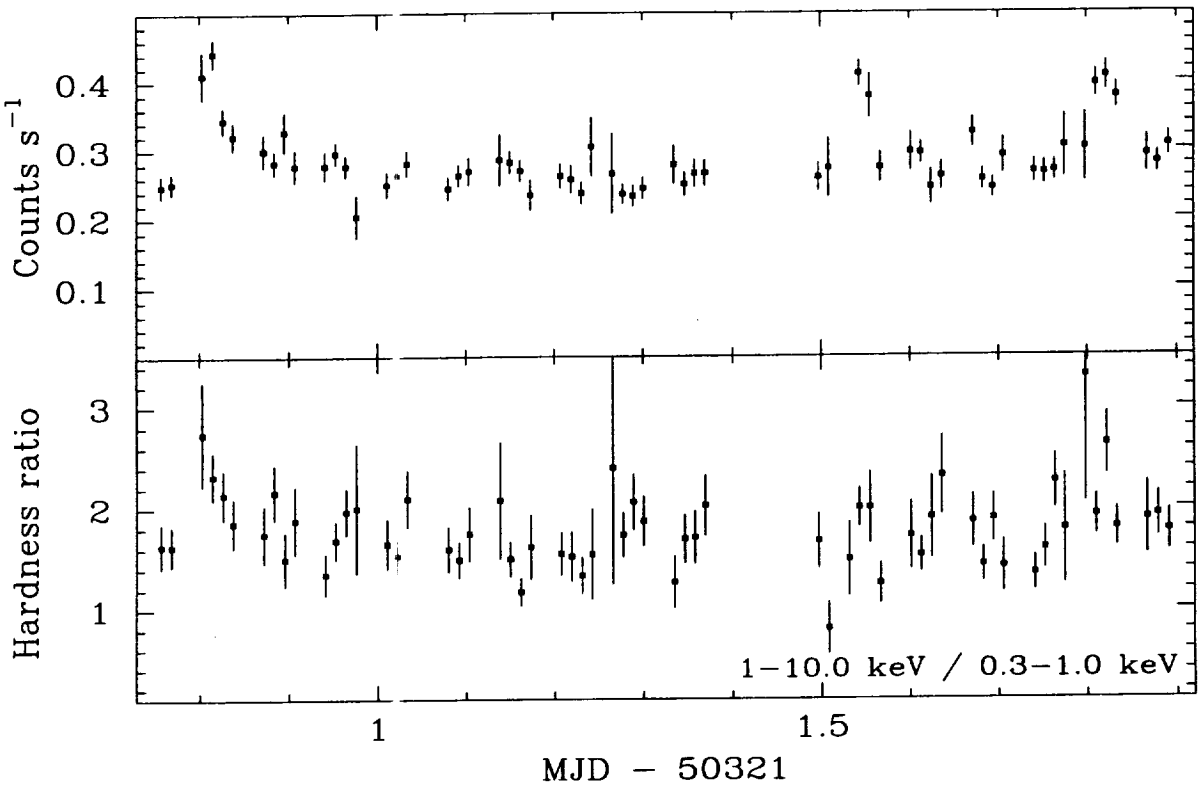

Fig. 1.— Top: the combined SIS and GIS 0.3–10 keV light curve for V471 Tau. Bottom: the hardness ratio between energy bands 0.3–1.0 keV and 1.0–10.0 keV.

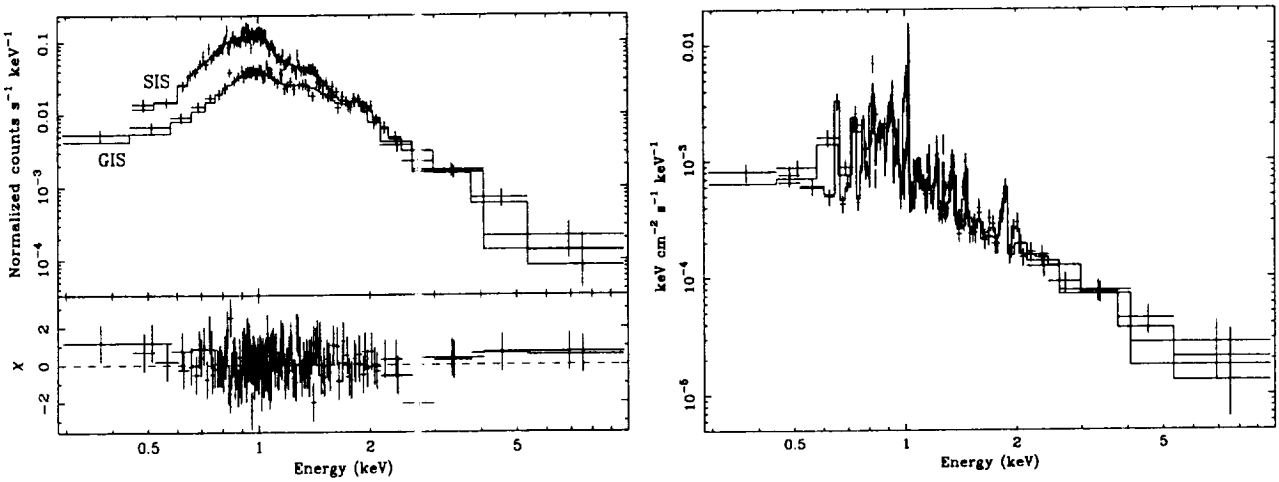

Fig. 2.— Left: The total combined GIS and SIS spectra of V471 Tau with best fit. The model is an absorbed, optically thin, two temperature thermal region corresponding to Model 4 in Table 1. Right: The data folded over the model.

TABLE 1

SPECTRAL FIT PARAMETERS FOR FOUR THERMAL MODELS. THE ABUNDANCE OF SOME OF THE ELEMENTS, HE, C, N, MG, AL, S, AR AND CA, WERE NOT WELL CONSTRAINED BY THE DATA. MODELS ARE IDENTICAL EXCEPT FOR DIFFERENT ASSUMED ABUNDANCES FOR THE ELEMENTS ABOVE. BEST FIT ABUNDANCES RELATIVE TO SOLAR FOR THE REMAINING TRANSITIONS IN THE ASCA BAND ARE PROVIDED FIRST, WITH THE TEMPERATURES AND EMISSION MEASURES, ASSUMING A TWO-TEMPERATURE EMISSION REGION, SECOND. THE χ^2 OF EACH FIT AND NUMBER OF DEGREES OF FREEDOM ARE PROVIDED AT THE BOTTOM.

Element	FIP (eV)	Model 1[a]	Model 2[b]	Model 3[c]	Model 4[d]
Ni	7.63	$0.31^{+0.21}_{-0.08}$	$0.10^{+0.15}_{-0.10}$	$0.21^{+0.57}_{-0.18}$	$0.01^{+0.66}_{-0.01}$
Fe	7.87	$0.31^{+0.21}_{-0.08}$	$0.25^{+0.11}_{-0.19}$	$0.43^{+0.23}_{-0.06}$	$0.60^{+0.24}_{-0.22}$
Si	8.15	$0.31^{+0.21}_{-0.08}$	$0.34^{+0.60}_{-0.17}$	$1.03^{+0.25}_{-0.28}$	$1.08^{+0.45}_{-0.04}$
O	13.61	$0.31^{+0.21}_{-0.08}$	$0.55^{+0.69}_{-0.37}$	$0.94^{+1.09}_{-0.34}$	$1.28^{+0.92}_{-0.92}$
Ne	21.56	$0.31^{+0.21}_{-0.08}$	$1.16^{+1.05}_{-0.58}$	$2.88^{+0.55}_{-0.95}$	$2.99^{+1.62}_{-0.84}$

Parameter	Model 1[a]	Model 2[b]	Model 3[c]	Model 4[d]
kT_1[e]	$0.78^{+0.03}_{-0.10}$	$0.74^{+0.04}_{-0.14}$	$0.69^{+0.08}_{-0.02}$	$0.69^{+0.07}_{-0.10}$
N_1[f]	$0.41^{+0.24}_{-0.07}$	$0.30^{+1.88}_{-0.12}$	$0.23^{+0.03}_{-0.08}$	$0.15^{+0.11}_{-0.02}$
kT_2[e]	$1.83^{+0.30}_{-0.15}$	$2.21^{+3.65}_{-0.63}$	$2.46^{+0.50}_{-0.54}$	$2.15^{+0.81}_{-0.28}$
N_2[f]	$0.35^{+0.48}_{-0.05}$	$0.15^{+0.28}_{-0.05}$	$0.18^{+0.02}_{-0.04}$	$0.27^{+0.03}_{-0.06}$
n_H[g]	$0.13^{+4.58}_{-0.13}$	$3.23^{+5.38}_{-3.23}$	$0.52^{+5.54}_{-0.52}$	$0.00^{+6.42}_{-0.00}$
χ^2(dof)	209(318)	196(313)	179(313)	174(313)

[a]Metal abundances all equal.

[b]Metal abundances equal to Fe, except Ni, Si, O and Ne.

[c]Metal abundances equal to solar, except Ni, Fe, Si, O and Ne.

[d]Metal abundances equal to the Hyades photospheric mean, except Ni, Fe, Si, O and Ne.

[e]Temperature (keV).

[f]Emission measure ($10^{53} \int n_e n_i dV$); n_e is the electron density, n_i the hydrogen density and dV the emitting volume. Source distance is taken to be 47 pc (Werner & Rauch 1997).

[g]Neutral column density (10^{20} cm^{-2}).

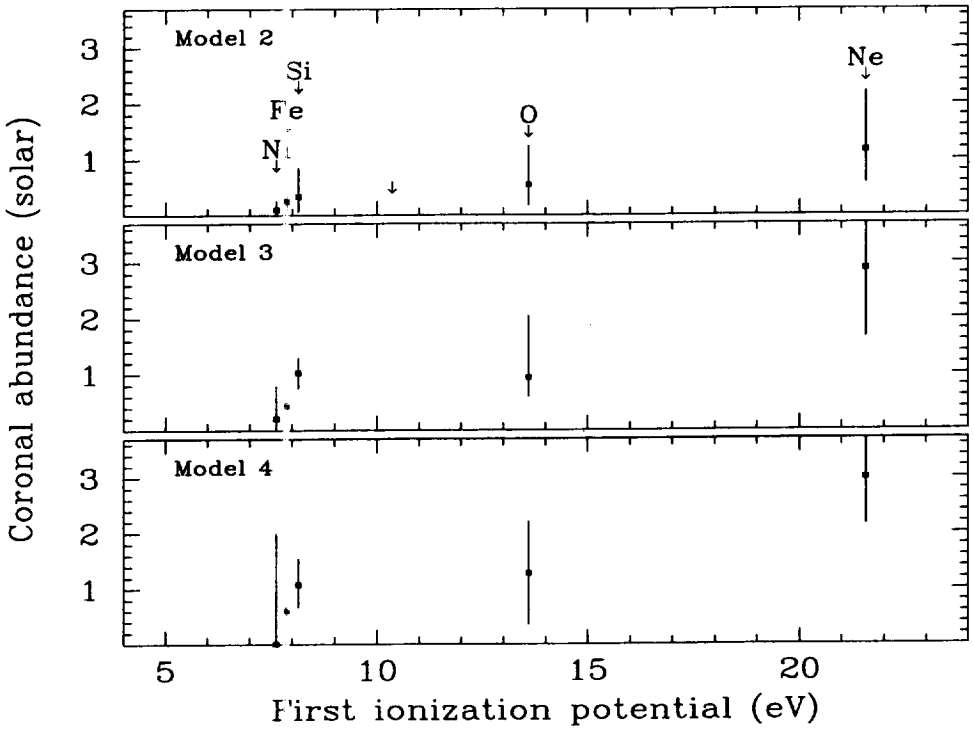

Fig. 3.— Elemental abundances from Models 2, 3 and 4, showing a relative overabundance of Ne in each case. Error bars are 90 percent confidence ranges.

model (Brickhouse et al. 2000), absorbed through a neutral interstellar column with photo-electric cross-sections provided by Balucinska-Church & McCammon (1992). Spectra from all four cameras were employed together to converge on a single model.

The currently public VAPEC code (version 1.10) does not include high n transitions of Fe XVII–XIX. Also there are systematic problems for the current set of Ni lines in this version. Therefore additional tables for Fe XVII; n = 6, 7 and 8 → 2, Fe XVIII; n = 6, 7 → 2 and Fe XIX; n = 6 → 2 are included plus a new table with corrected Ni ionization balances, as described in Brickhouse et al. (2000).

If all abundances are allowed to roam as independent free fit parameters, then statistically significant constraints on any individual element are not possible. Counting statistics are not sufficient to constrain the abundances of all the elements that emit in the *ASCA* energy band. By trial and error we find that significant detections of Ni, Fe, Si, O and Ne are made if we make some reasonable assumptions concerning the fractions of the other elements contributing to the line spectrum, i.e., C, N, Mg, Al, S, Ar and Ca. Consequently we describe below four abundance models.

Model 1 assumes the abundances of all the metals are equal; in this case the abundance is dominated by the L shell lines of Fe. Model 2 allows the abundances of Ni, Si, O and Ne to float as free parameters while the others are assumed equal. The combined metal abundance will again be dominated by Fe. Model 3 is similar to model 2 except that the Fe abundance is decoupled from the combined elements and allowed to float as a further independent free parameter. The remaining abundances of He, C, N, Mg, Al, S, Ar and Ca are fixed constant at their solar values. Model 4 is identical to model 3 except our fixed abundances have the mean photospheric value of the Hyades members ([m/H] = +0.1; Martín, Pavlenko and Rebolo 1997).

Realistically we expect a whole range of plasma temperatures and, unsurprisingly, single-temperature models provide poor fits to the data. Two-temperature models yield statistically significant fits although they are still undoubtedly a simplification of the temperature structure. Table

1 lists the best fit parameters and χ^2 statistic for each model. Between Models 2, 3 and 4 we find consistency between temperatures and emission measures. Since the source is in the galactic neighbourhood, it is gratifying to find that, within uncertainties, the neutral column density is both consistent with zero and smaller than the total galactic column in that direction ($1.58\text{E}\times10^{21}$ cm^{-2}; Dickey & Lockman 1990). In each case we find an inverse First Ionization Potential (FIP) effect, i.e., abundances increase as a function of FIP. In all cases, Fe abundance is significantly subsolar, the opposite to the solar corona, whereas Ne is greater than solar, significantly so in Models 3 and 4.

On the left-hand side of Fig. 2 we show the best-fit model 4, folded on the energy-resolved count rate and it's residuals. On the right, the data is folded over the best-fit model. To increase clarity, both SIS0 and SIS1, and GIS2 and GIS3 spectra have been combined. The coronal abundances of the five significantly-constrained elements are plotted against FIP in Fig. 3.

4. Discussion

We have determined, albeit with a few model assumptions, the element abundances of Ni, Fe, Si, O and Ne in the corona of V471 Tau and demonstrated an abundance increase with FIP compared to the solar photospheric values. In the following section, we ask whether we expect to find fossil abundances from the post common envelope epoch. We also discuss the proposed mechanism behind the FIP effect and, finally, compare the coronal abundances with the measured photospheric abundances of dwarf stars in the Hyades cluster.

4.1. Common envelope abundances

During the white dwarf progenitor's red giant phase of evolution, the two stars shared a common envelope and, therefore, there was element mixing between them. Using LTE atmosphere fits to optical spectroscopy of V471 Tau, and providing NLTE corrections, Martín et al. (1997) found photospheric abundances consistent with the Hyades, [m/H] = +0.1, in Al, Ca, Fe and Si. The one exception was Li, where $\log \text{N}_{\text{Li}} = 2.4 \pm 0.3$. This is greater than a factor 10^2 more abundant than normal Hyades members. Although Li is usually depleted in convection layers, Martín et al. argue that the rapid rotation of the K star maintains the fossil level of Li after sharing a common envelope phase with the Li-rich giant (de la Reza, Drake & da Silva 1996). Unfortunately there are no Li transitions in the *ASCA* energy band to test this independently.

Marks & Sarna (1998) calculate the evolution of photospheric abundances on the companion star of cataclysmic variables, including the effects of a common envelope epoch. They indicate that, indeed, photospheric abundances in the K star are expected to remain unchanged through the common envelope phase, and remain constant thereafter until the white dwarf accretion rate is sufficient to drive a cycle of nova eruptions. Therefore we do not expect to find evidence for the common envelope phase in the current measurements, however, peculiar abundances may yet be present if the proposed *IUE* detection of expanding nova material around V471 Tau by Bruhweiler & Sion (1986) and Sion et al. (1989) is confirmed. However subsequent *HST* spectroscopy shows no indication of shell features but does detect transient coronal ejection events (Bond et al. 2001). These may well have been mistaken for an expanding shell before coronal ejections were time-resolved by *HST*. In light of both the observational and theoretical evidence, we will assume that the photospheric abundances of the companion star in V471 Tau are identical to the average Hyades dwarf.

4.2. The FIP effect

Observations have indicated that the coronal abundances in the sun are different from the solar photosphere (Meyer 1985a,b). This is probably equally true for active stars (Brinkman et al. 2001). While in most of cases the photospheric abundances remain uncertain, there is at least one strong piece of evidence for vertically-stratified abundances in stellar sources. It derives from the fact that stellar abundances are correlated with elemental FIP. In the solar atmosphere the ratio of coronal to photospheric abundances decreases with FIP. When comparing stellar coronal abundances to the solar photosphere some sources follow this trend while others show the "inverse FIP effect", i.e. an increasing ratio with

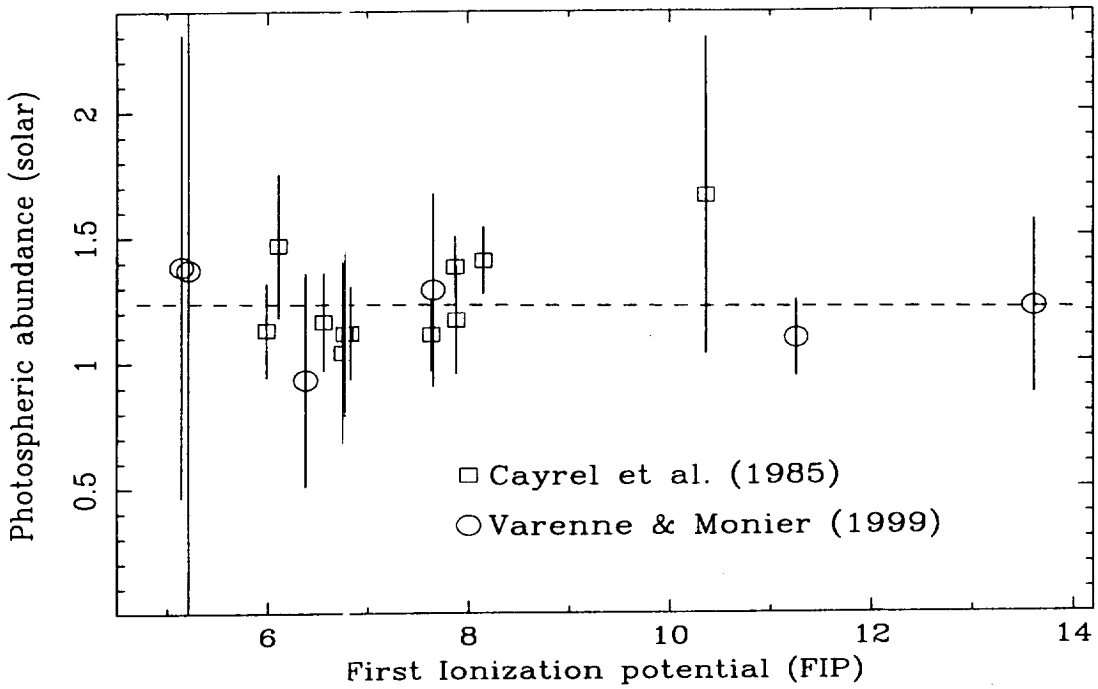

Fig. 4.— Mean photospheric abundances of Hyades dwarfs (Cayrel et al. 1985; Varenne & Monier 1999) plotted as function of FIP. The line is the best linear fit to the data.

increasing FIP (Brinkman et al. 2001).

Abundances in most stellar photospheres are not well known. Instead, it is common practice to compare stellar coronal abundances with the solar photosphere. The correlation of this ratio as function of FIP has been observed to change during X-ray flares. Audard, Güdel & Mewe (2001) find an inverse FIP affect in HR 1099 during quiescence but a direct FIP effect during flares. These events are thought to be directly associated with the process of element fractionation in stellar atmospheres (Wang 1996). Charged particles are accelerated along field lines in loops above the stellar photosphere. Elements with differing FIPs will be ionized by differing amounts. Low FIP material has a higher probability of being accelerated along magnetic loops and diffused into the chromosphere. Consequently there is a higher abundance of high FIP particles remaining in the lower atmosphere which are lifted into the corona by flare ejections (Schmelz 1993).

4.3. Abundances in the Hyades

Rather than adopting solar abundances, ideally we would prefer to have direct measurements of photospheric abundances in order to make an unbiased comparison between photosphere and corona. These are poorly determined generally because of uncertainties in galactic element mixing and the details of stellar spectral synthesis models. Fortunately V471 Tau is a member of the nearest open cluster, the Hyades (Werner & Rauch 1997), where photospheric abundances are considerably better determined than most coronal X-ray sources.

Metallicities in open clusters are indicators of the quantity and rate of chemical mixing in the galaxy. However stellar abundance determinations are generally plagued by a wide range of biases (see e.g. Griffin & Holweger 1989). Various techniques have consequently supplied abundances for the Hyades cluster ranging from [Fe/H] = −0.09 (Tomkin & Lambert 1978) to [Fe/H] = +0.42 (Gustafsson & Nissen 1972).

Although not unequivocally free of bias, the most careful abundance measurement has been performed by Cayrel, Cayrel de Strobel & Campbell (1985). They determine a mean [Fe/H] enhancement over solar of $+0.12 \pm 0.03$ using high dispersion spectroscopy of a sample of 12 Hyades

dwarfs distributed tightly about the solar spectral type. This result was determined by comparison of the curve of growth over the linear and saturated branches of FeI lines with photospheric spectral models.

A large surface fraction of active regions over these stars would probably result in an underestimate of the abundance, but an identical estimate of [Fe/H] = $+0.14 \pm 0.01$ from a smaller sample of FeII lines suggests that any bias due to chromospheric activity is small among the measured cases. While systematic errors may still be present, this result has been confirmed with a sample of F stars with $v \sin i < 30$ km s^{-1} by Boesgaard (1989), finding [Fe/H] = $+0.13 \pm 0.03$. Consequently, by comparison with the *ASCA* results, Fe abundance is constant between the photosphere and corona of V471 Tau, within the uncertainties.

Cayrel et al. (1985) also provide coronal abundances for NiI, and SiI; [Ni/H] = $+0.07 \pm 0.05$ and [Si/H] = $+0.16 \pm 0.04$. Varenne & Monier (1999) present photospheric O abundances for 26 F stars in the Hyades with an average value of [O/H] = +0.07, compared to the solar values of Grevesse & Noels (1993).

Because of the systematic and measurement uncertainties in the *ASCA* data it is perhaps unwise to make meaningful comparisons between the corona and photosphere populations of individual species. However a comparison of the general FIP distributions in the three coronal models versus the photospheric abundances shows a consistent difference. We combine the Hyades abundances from Cayrel et al. and Varenne & Monier in Fig. 4. A linear least-squares fit reveals a slope of 0.00 ± 0.05, where the error is the 90 percent confidence limit, i.e. the abundances are consistent with a flat distribution across the range of FIP. The mean metallic abundance is 1.2 ± 0.1 solar. Critically, photospheric Ne has not bean measured in the Hyades because only high-ionization species emit brightly in the optical band. We therefore measure the slope of the X-ray distributions both with, and without, Ne included. With Ne, least-square fitting yields slopes of 0.09 ± 0.08 (Model 2), 0.15 ± 0.10 (Model 3) and 0.17 ± 0.13 (Model 4). Consequently, the coronal FIP distribution is significantly steeper than the Hyades mean. However, without Ne, we have 0.10 ± 0.15 (Model 2), 0.15 ± 0.20 (Model 3) and 0.13 ± 0.24 (Model 4). In these cases there are no significant differences between the coronal and photospheric populations.

5. Conclusion

We have measured model-dependent coronal abundances of Ni, Fe, Si, O and Ne in the corona of the post-common envelope binary V471 Tau. A single-temperature plasma model does not fit the data adequately. Binary evolution calculations have predicted that we would see no symptoms of element mixing during the common-envelope epoch and we indeed find no evidence for it; i.e., abundances are not unusual compared to the coronae of single stars or wide binaries. In all the models considered, the coronal Fe abundance is significantly less than the Hyades photospheric mean. This is in direct contrast to the ratio of Fe in the solar corona which is overabundant relative to the solar photosphere. There is evidence for an inverse FIP effect, although this relies entirely on our measurement of Ne abundance. Due to the lack of low-ionization Ne lines in the optical band, the photospheric abundance of this element cannot be directly compared to the coronal value, adding further uncertainty. While CCD spectroscopy is not currently an ideal method for abundance determination, these data indicate that V471 Tau is a viable and interesting target for the grating instruments on-board the *Chandra* and *XMM-Newton* observatories.

This paper was based on data obtained from the High Energy Astrophysics Science Archive Research Center (HEASARC), provided by NASA's Goddard Space Flight Center. We thank Nancy Brickhouse for supplying additional Fe and Ni transition data.

REFERENCES

Audard M., Güdel M., Mewe R., 2001, A&A, 365 L318

Balucinska-Church M., McCammon D., 1992, ApJ, 400, 699

Boesgaard A.M., 1989, ApJ, 336, 798

Bond H.E., Mullan D.J., O'Brien M.S., Sion E.M., 2001, ApJ, 560, 919

Brickhouse N.S., Dupree A.K., Edgar R.J., Liedahl D.A., Drake S.A., White N.E., Singh K.P., 2000, ApJ, 530, 387

Brinkman A.C. et al., 2001, A&A, 365, L324

Bruhweiler F.C., Sion E.M., 1986, ApJ, 304, L21

Burke B.E. et al., 1991, IEEE Trans., ED-38, 1069

Cayrel R., Cayrel de Strobel G., Campbell B., 1985, A&A, 146, 249

de la Reza R., Drake N.A., da Silva L., 1996, ApJ, 456, L115

Dickey J.M., Lockman F.J., 1990. ARA&A, 28, 215

Drake S.A., 1996, p. 215 in Holt S S., Sonneborn G., eds., in Proceedings of the sixth (6th) annual October Astrophysics Conference in College Park, Maryland, ASP Conference Series Vol. 99

Grevesse N., Noels A., 1993, Physica Scripta T., 47, 133

Griffin R.E.M., Holweger H., 1989, A&A, 214, 249

Gustafsson B, Nissen P.E., A&A, 19, 261

Jensen K.A., Swank J.H., Petre R., Guinan E.F., Sion E.M., Shipman H.L., 1986, ApJ, 309, L27

Marks P.B., Sarna M.J., 1998, MNRAS, 699, 720

Martín E.L., Pavlenko Y., Rebelo F., 1997, A& A, 326, 731

Meyer J.-P., 1985a, ApJS, 57, 151

Meyer J.-P., 1985b, ApJS, 57, 173

Nelson B., Young A., 1970, PASP, 82, 699

Ohashi T. et al., 1991, Proc. SPIE 1549, 9

Paczýnski B., 1976, p. 75 in Eggleton P., Mitton S., Whelan J., eds., Structure and Evolution of Close Binary Systems, IAU Symposium no. 73, Reidel: Dordrecht

Schmelz J.T., 1993, ApJ, 408, 373

Schmitt J.H.M.M., Haisch B., Barwig H., 1993, ApJ, 419, L81

Serlemitsos et al., 1995, PASJ, 47, 105

Sion E.M., Bruhweiler F.C., Mullan D., Carpenter K., 1989, ApJ, 341, L17

Taam R.E., 1983 ApJ, 268, 361

Tanaka Y., Inoue H., Holt S.S., 1994, PASJ, 46, L37

Tomkin J., Lambert D.L., 1978, ApJ, 223, 937

Tsikoudi V., Kellet B.J., 2000, MNRAS, 319, 1147

van Buren D., Charles P.A., Mason K.O., 1980, ApJ, 242, L105

Varenne O., Monier R., 1999, A&A, 351, 247

Wang Y.-M., 1996, ApJ, 464, L91

Warner B., 1995, Cataclysmic Variable Stars, CUP: Camridge

Werner K., Rauch T., 1997, A&A, 324, L25

Wheatley P.W., 1998, MNRAS, 297, 1145

Young A., Klimke A., Africano J.L., Quigley R., Radick R.R., van Buren D., 1983, ApJ, 267, 655

This 2-column preprint was prepared with the AAS LaTeX macros v5.0.